Journal of Medical Devices Technology
jmeditec.utm.my

Original Research

An Investigative Analysis of RFID Read Range Under Human Proximity with Different Body Mass Index

Faishal Adilah Suryanata[1,2], Raimi Dewan[1,2,3*], DiviyaDevi Paramasivam[2,3], and Naufal Fikri Muhammad[1,2]
[1] Department of Biomedical Engineering and Health Sciences, Faculty of Electrical Engineering, Universiti Teknologi Malaysia, Johor, Malaysia
[2] Advanced Radio Frequency & Microwave Research Group, Faculty of Electrical Engineering, Universiti Teknologi Malaysia, Johor, Malaysia
[3] IJN-UTM Cardiovascular Engineering Centre, Institute of Human Centred Engineering, Universiti Teknologi Malaysia, Johor, Malaysia

ARTICLE INFO

Article History:
Received 17 August 2023
Accepted 26 May 2024
Available online 30 June 2024

Keywords:
BMI,
Free space,
Human tissue layer,
Open-field measurement,
Read range,
RFID

ABSTRACT

Radio Frequency Identification (RFID), application technology is implemented to enhance the efficiency of service through the integration of data automatically. RFID is a data transmission technology comprising interconnected tags and readers designed to facilitate the exchange of information. The human tissue layer appears to have an influence on the RFID read range performance. The aim of this study is to examine and analyse the read range performance under two conditions: in a free-space setting and when placed on a human body model. Body Mass Index (BMI) serves as a requirement for studying its effect of fat layer thickness. The results reveal that the commercial RFID read range may be maximized up to 5.3 meters in open space as per specification and decreases depending on the human body model and varied fat layer thickness. The collected information evaluated using the CST studio Suites 2021 Student Version Software and an open-field experiment with participants with varying BMIs.

INTRODUCTION

The Internet of Things (IoT) is rapidly being used in a variety of industrial settings. This technology can successfully increase job productivity, work efficiency and provide users with personalized information or services. RFID-based solutions have been adopted due to the benefits of simultaneous identification and placement (Xu et al., 2023). RFID applications may additionally relate to healthcare IoT functionalities to increase flexibility in connecting broad healthcare systems which consisted of various wirelessly connected devices. RFID technology facilitates the regular maintenance, and traceability of crucial health assets, ensuring reliable functionality assessment and contributes to enhance the patient safety. In the realm of medical informatics, RFID assumes a prominent role in the accurate identification and retrieval of patient-specific medical records, containing crucial personal health information (Mohammad et al., 2022). RFID tags are often mounted to the object to be evaluated to identify it. However, RFID can be influenced by external factors in some practical situations (Xiang et al., 2022).

The latest scientific research shows that the presence of a human body in close proximity significantly affects the performance of RFID antennas, resulting in limited reading capabilities (Tajin et al., 2021). When integrated into garments, the RFID tag might function consistently (Gmih & Farchi, 2020). The RFID tag antenna performs well in free space. However, on-body performance is severely limited due to lower radiation efficiency triggered by the loss of power in the body of an individual (Tajin et al., 2021). The development of a fitness tracker that is physically associated with the body of an individual is projected (Miozzi, 2020). As a consequence, the repercussions of the human body's lots of tissue layers, consisting of skin, fat, and muscle, on read range performance are being investigated. The electrical properties of human body parameters as gathered from the datasheet presented in Table 1 are necessary as references in the study. In this study, it is crucial

* Raimi Dewan (raimi.dar@utm.my)

Department of Biomedical Engineering & Health Sciences, Faculty of Electrical Engineering, Universiti Teknologi Malaysia, 81310 UTM Johor Bahru, Johor, Malaysia.

to analyze the performance variation in read range between the free space condition and the human body model. CST Studio Suites 2021 student version is used to simulate the RFID tag read range as the reference for the open-field experiment. Human body layer design would link to a database of human body electrical characteristics for design and would use CST software to simulate RFID performance on a human body model.

Table 1 Human body electrical properties

Body Part	Sub Body Part	Thickness (mm)	Permittivity	Conductivity (S/m)	References
Arm	Skin	1.5	41.32	0.855	(Casula & Montisci, 2019)
	Fat	20	5.46	0.05	
	Muscle	30	54.97	0.934	
General	Skin	1.7	-	-	(Yalduz et al., 2020)
	Fat	8	-	-	
	Muscle	10	-	-	
Arm, leg	Skin	2	-	-	(Nie et al., 2021)
	Fat	5	5.27	0.11	
	Muscle	20	52.67	1.77	(Farahat, 2021)
Chest or stomach	Skin	2	36.06	2.84	(Farahat, 2021)
	Fat	4	5.03	0.23	
	Muscle	5	49.84	3.93	
General	Skin	1	38.007	1.49	(Bo Yin, 2021)
	Fat	5	5.28	0.11	
	Muscle	20	52.729	1.77	
Chest or arm	Skin	2	35	3.8	(Keshwani et al., 2021)
	Fat	5	4.95	0.3	
	Muscle	20	48.4	5.12	
Chest, leg, arm	Skin (wet)	1	49.9	-	(Wissem El May, 2021)
	Fat	5	5.58	-	
	Muscle	40	57.13	-	

MATERIAL AND METHODOLOGY

In this part, the details of tools and the methodology to achieve the study objectives are explained. This part begins with the explanation of RFID system and human body model. The abdomen part was used as the main focus of this study. The abdomen was chosen as the preferred focus of experiment because has visible variations across diverse BMI ranges. The read range and BMI formula also included as the study references.

RFID System

The RFID sensor system consists of an RFID tag combined with an RFID reader, facilitating the transmission of data. The element known as the antenna establishes the interaction between the RFID tag and the reader (Xiang et al., 2022). RFID tags can be divided into distinct groupings, specifically passive and active RFID tags. Active RFID tags are endowed with an integrated power source, commonly a battery, facilitating autonomous operation. On the other hand, passive RFID tags operate devoid of battery requirements, relying upon external RF signals for both power and data transmission (Gao & Lu, 2022).

Passive RFID tags offer the advantages of not requiring maintenance, more affordable, and have great lifespan due to battery less operation. The reader transmits a specific frequency of signal through the transmitting antenna when interrogating a passive RFID tag. Upon tag transmission to the antenna, an induced current is present, and the energy required for signal transmission can be derived from this current (Gao & Lu, 2022). The tag chip functions through modification of the signal data. Passive RFID technologies can be classified in accordance with the frequency of operation of RFID tags, which can be a low-frequency (LF) at 125 kHz, high-frequency (HF) at 13.56 MHz, or ultra-high-frequency (UHF) with a frequency range of 860-960 MHz. The variance between UHF bands of frequency is defined by national regulations (Xiang et al., 2022).

The 9662 RFID tag model with the standard EPC Class 1 Gen 2 (RichAfid, n.d.). As displayed in Figure 1, it selected as the commercial RFID tag model to be replicated and simulated in CST software before being executed for the read range in the open-field experiment. The RFID tag model functions within the frequency range of 860-960 MHZ, exhibiting a read range from 5.0 meter until 6.0 meter. 70 mm x 17 mm antenna supported on the RFID tag using Alien Higgs-3 as the chip. The antenna is constructed using PET as the substrate material with dimension 83± 1 mm (RichAfid, n.d.). Figure 2 represents the implementation of a Chainway C72 UHF RFID reader with dimensions 164.2 x 80.0 x 24.3 mm and 654 g as the weight will be used in the open-field measurement analysis. The RFID reader operates using Android 6.0 and Java as the programming language. Several frequencies can be detected using this RFID reader model such as 865 until 868 MHz, 920-925 MHz, and 902-928 MHz with referring to the protocol of EPC C1 Gen 2 or ISO 18000-6C (Chainway, n.d.).

Fig. 1 9662 RFID tag model

Fig. 2 Chainway C72 UHF RFID reader (Stopforth, 2021)

Human Body Model

The primary constraints affecting body-worn antennas are associated with the electrical properties of the human body, encompassing factors like permittivity and conductivity. Consequently, the presence of the human body layer can exert a considerable adverse impact on antenna performance. Therefore, the human body layer is critically important for optimizing the antenna. The human model implemented in the most recent study referred to the skin, fat, and muscle layer. From an electromagnetic standpoint, all of the layers are lossy dielectrics with varying thicknesses and frequency complex permittivity (Ahmed et al., 2019). The electrical properties of human body parameters as gathered from the datasheet presented in Table 2 are necessary as references in the study. According to further research obtained from a respectable publication, abdominal electrical tissue differentiated with certain BMI categorization was chosen as the body component. Table 4 shows the electrical characteristics of the abdomen in relation to BMI.

Table 2 Human abdomen electrical properties

Body Part	Sub Body Part	BMI	Thickness (mm)	Permittivity	Conductivity (S/m)	References
Abdomen	Fat	Underweight	12	911.5	0.042	(Chu, 2022), (Sakai, 2023)
	Fat	Normal	36	911.5	0.042	
	Fat	Overweight	47	911.5	0.042	
	Fat	Obese	64	911.5	0.042	

Read Range

The RFID tag read range is the range of maximum distance that an RFID reader is capable of reading and is extremely important in RFID applications (Bansal et al., 2022). The read range of passive RFID tags is impacted by the frequency of operations, the specific type of reader and tags, disturbance, and the condition of the surroundings. (Tsalapati et al., 2021). The equation 1 is the formula used to calculate read range accurate measurements. (Bansal et al., 2022),

$$R_{max} = \frac{\lambda}{4\pi}\left(\frac{P_{EIRP}G_r\tau}{P_{ic}}\right)^{1/2} = \frac{\lambda}{4\pi}\left(\frac{P_{EIRP}G_r\tau}{P_{tag}}\right)^{1/2} \quad (1)$$

where λ signifies the bandwidth in free space corresponding to the operating frequency of the reader, while $P_{EIRP} = P_{tx}G_{tx}$, denoted as the product of P_{tx} (RFID reader's transmitted power) and G_{tx} (RFID reader's gain), represents the aggregate effective radiated power. Moreover, τ symbolizes the power transmission coefficient of the RFID tag, and P_{ic} stands for the sensitivity of the RFID chip (Bansal et al., 2022).

Body Mass Index (BMI)

Body Mass Index (BMI) is an indicator and credible anthropometric methodology that assists in determining the proportion of body fat and reviewing a person's nutritional and health state (Mohajan & Mohajan, 2023). BMI measurement is referring to the BMI range divisions such as underweight (< 18.5 kg/m^2), normal (18.5 – 24.9 kg/m^2), overweight (25 - 29.9 kg/m^2), and obese (30 and higher) (Soeroto AY, 2020). The formula is offered by equation 2 whereas weight and height are included in the calculation (Chatterjee, 2020),

$$\text{BMI} = \text{Weight} / \text{Height}^2 \quad (2)$$

RESULTS AND DISCUSSION

The study outcome provides specific information in this part while also making references to the electrical characteristics of the abdomen and the technical specifications of the RFID tag and reader. The collection of data on the electrical properties of the abdomen focuses on various BMI categories, including underweight, normal, overweight, and obese. The abdomen part has been selected for analysis and investigation of the impact on the RFID read range performance through software simulation and open-field experiment.

Free space

RFID tag is set up in the free space design environment, which is an empty area with no interference. Before commencing the simulation operation, the 9662 RFID tag model must be replicated. The S11 parameter is crucial in order to efficiently simulate the read range where it is for maximizing the dimensions of the RFID tag model. After the RFID tag model has been optimized using the S11 parameter, it could potentially be processed for read range analysis for confirmation of maximum read range as per specification. Figure 3 illustrates the front structure of the RFID tag replication model, while Figure 4 presents the back view of the design.

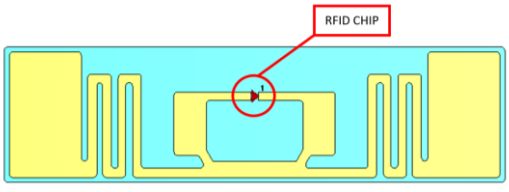

Fig. 3 RFID tag front view of the design replication

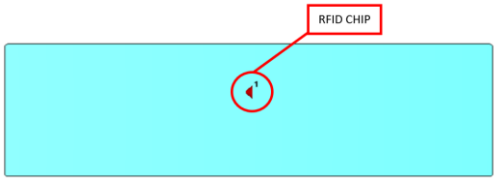

Fig. 4 RFID tag back view of the design replication

Read Range

The Read Range (RR) inspection is carried out under two conditions: in free space and on a human body model. Figure 5 illustrates a graphical representation of the read range in free space conditions. At a frequency of 910 MHz, the graph displays a peak distance of 5.3 meters, encompassing a range from 5.0 to 5.5 meters. The read range reported is comparable with the datasheet, which shows that with the frequency ranges 902-928 MHz and 865-868 MHz, the RFID tag read range can possibly be encouraged about 5.0 to 6.0 meters. In human body context, the proximity of the RFID tag to the body directly influences the read range which is affected by the body's specific characteristics (Suryanata et al., 2023).

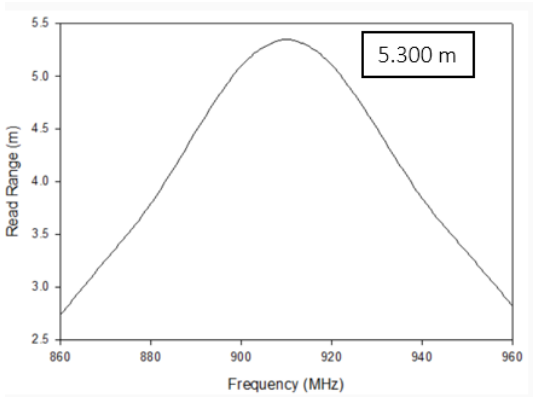

Fig 5. Free space condition read range graph

The human body model (abdomen) was developed with the CST software, which is linked to the design replication of the 9662 RFID tag. The design of the human body model necessitated the specification of tissue layer thickness, permittivity, and conductivity as essential factors. With an increase in Body Mass Index (BMI), resulting in varying fat layer thickness, the read range performance of RFID is diminished. Each BMI category corresponds to varying levels of body fat. As caloric intake increases, adipose tissues expand and contribute to higher body fat percentages. Conversely, a reduction in BMI correlates with the accelerated metabolic processes, which leads to the use of stored energy, and the reduction of adipose tissues. Body fat is also influenced by an individual's age and sex (Jeong et al., 2023). Due to higher body fat percentages, the individual's BMI influences the performance of RFID tag read range. Figure 6(a) presents an underweight BMI fat layer of the abdomen tissue with a thickness of 12 mm, and Figure 7(a) demonstrates a simulated Read Range (RR) graph. The influence of the underweight human tissue layer seems to reduce the RR to 0.4400 m with 169% differences with free space condition. Figure 6(b) indicates a normal fat layer with the thickness of 36 mm and the RR reduces to 0.2062 m or 185.021% differences with free space condition, as apparent in Figure 7(b). Figure 6(c) outlines an overweight model with more fat thickness about 47 mm, resulting in a reduction in the RR that having 185.076% difference with free space condition or decreases to 0.2054 m in Figure 7(c). The obese fat layer has the largest fat layer with 64 mm as demonstrated in Figure 6(d) and reduces the RR until -18.2100 m according to Figure 7(d). Based on the simulation graph analysis, the read range decreased further as the fat layer increased. Figure 8 illustrates a comparison of RR performance in free-space condition and on individuals with different BMI, with reference to Malaysian frequency specification (910-920 MHz).

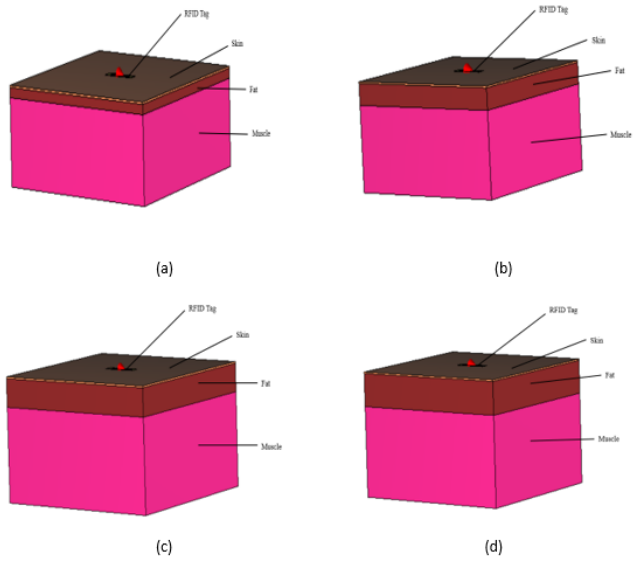

Fig. 6 The Abdomen tissue layer of underweight BMI with fat layer about 12 mm (a), normal BMI with 36 mm (b), overweight 47 mm (c). and obese with 64 mm (d)

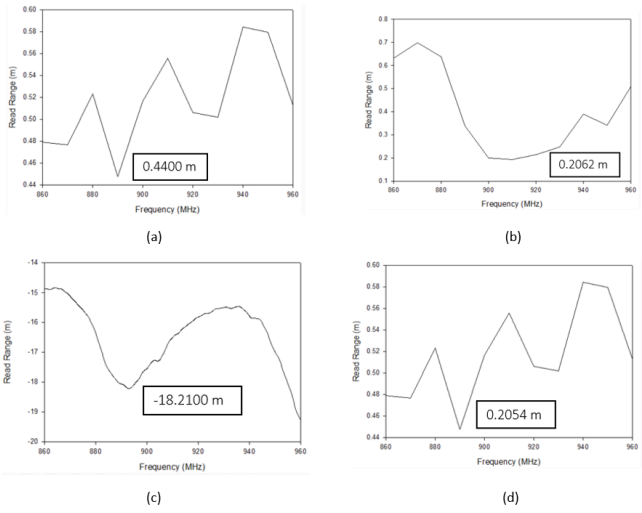

Fig. 7 Underweight BMI simulated read range graph with the maximum value at 0.4400 meters (a), normal BMI simulated read range at 0.2062 m (b), obese BMI simulated read range graph at -18.21 m (c), overweight BMI simulated read range graph at 0.2054 m (d)

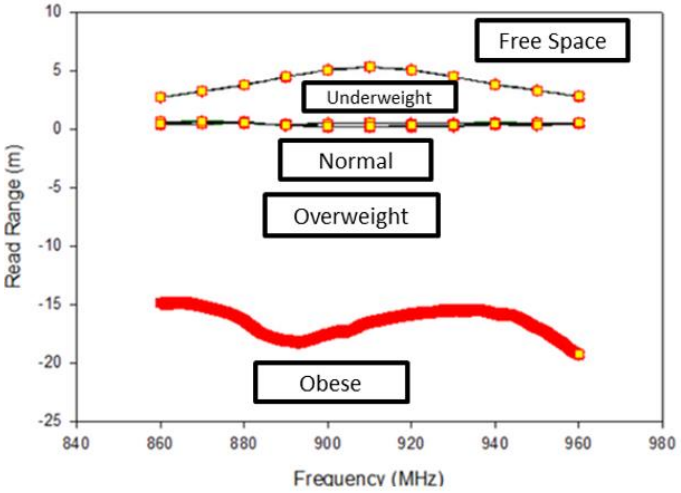

Fig. 8 Comparation graph of read range performance between in free-space condition and on individuals with various BMI referring to Malaysian frequency specification

Open-Field Measurement Analysis

The open-field experiment can be conducted by utilizing the CST software to stimulate the read range (RR). The simulation and measurement are not directly correlated because the exact permittivity and thickness of the tissue layers are unknown for individuals with varying BMI. The average permittivity and thickness were used only for reference comparison. The comparison would be used to analyze the curve characteristic between the measured results. The RFID tag was attached to the abdomen of four people with varying BMIs such as underweight, normal, overweight, and obese during the experiment, as illustrated in Figure 9. Figure 10 illustrates the open-field measurement settings of RR by attaching the RFID tag on the subject. To examine the variances in RR between different countries, this study required the use of a variety of frequencies including Malaysia (910-920 MHz), Thailand (920-925 MHz), Indonesia (923-925 MHz), Singapore (920-925 MHz), Vietnam (920-923 MHz), and the United States Standard (902-928 MHz) (Limited, 2024; NF. Miswadi, 2022; Technologies, 2022). Table 3 presents the RR data of the RFID tag in free space conditions with different frequency ranges. On average, across all frequency ranges, the RR signifies that the RFID tag can be detected at a distance of 6 m, which aligns with the RR specified in the RFID tag datasheet, ranging from 5 to 6 m range. When the RFID tag was attached to a human model representing an underweight BMI, as shown in Table 4, The RR decreased significantly to an average of 0.3283 m, exhibiting a 179 % reduction compared to the free space condition. In the case of normal BMI, presented in Table 5, the RR decreased to 0.2733 m, indicating a 182% reduction due to the increased thickness of the fat layer. Table 6 demonstrates that the individuals with an overweight BMI, the read range further decreased to 0.1766 m, reflecting a 188 % reduction compared to free space condition. Finally, in Table 7, for the obese BMI category, the RR decreased to 0.1183 m, indicating a reduction of 192 % compared to free space condition. The RR performance is influenced by the thickness, permittivity, and conductivity of the human body layer, wherein the fat layer thickness plays a notable role. Without barriers such as the human body, metal, or other conductive materials, the RR can be substantially prolonged in free space. Furthermore, minor variations in RR reading performance may arise due to discrepancies in frequency ranges adopted by different nations (Suryanata, 2023). Within the table structure, the symbol denoted by "/" representing the RFID tag readability through the

Table 3 Free space condition open-field experiment

No.	Read Range Distance (meter)													
	7.0	**6.5**	**6.0**	**5.5**	**5.0**	**4.5**	**4.0**	**3.5**	**3.0**	**2.5**	**2.0**	**1.5**	**1.0**	**0.5**
Malaysia (910-920 MHz)	x	x	/	/	/	/	/	/	/	/	/	/	/	/
Thailand (920-925 MHz)	x	x	/	/	/	/	/	/	/	/	/	/	/	/
Indonesia (923-925 MHz)	x	/	/	/	/	/	/	/	/	/	/	/	/	/
Singapore (920-925 MHz)	x	x	/	/	/	/	/	/	/	/	/	/	/	/
Vietnam (920-923 MHz)	x	x	/	/	/	/	/	/	/	/	/	/	/	/
United States (902-928 MHz)	x	x	/	/	/	/	/	/	/	/	/	/	/	/
Total Average	6 meter													

RFID reader, whereas "x" symbol indicates the incapacity of the RFID tag to be detected by the reader.

Table 4 Underweight BMI condition open-field experiment

No.	Read Range Distance (meter)													
	7.0	**6.5**	**6.0**	**5.5**	**5.0**	**4.5**	**4.0**	**3.5**	**3.0**	**2.5**	**2.0**	**1.5**	**1.0**	**Less than 1.0**
Malaysia (910-920 MHz)	x	x	x	x	x	x	x	x	x	x	x	x	x	0.3300
Thailand (920-925 MHz)	x	x	x	x	x	x	x	x	x	x	x	x	x	0.3300
Indonesia (923-925 MHz)	x	x	x	x	x	x	x	x	x	x	x	x	x	0.3200
Singapore (920-925 MHz)	x	x	x	x	x	x	x	x	x	x	x	x	x	0.3300
Vietnam (920-923 MHz)	x	x	x	x	x	x	x	x	x	x	x	x	x	0.3300
United States (902-928 MHz)	x	x	x	x	x	x	x	x	x	x	x	x	x	0.3300
Total Average	0.3283 meter													

Table 5 Normal BMI condition open-field experiment

No.	Read Range Distance (meter)													
	7.0	**6.5**	**6.0**	**5.5**	**5.0**	**4.5**	**4.0**	**3.5**	**3.0**	**2.5**	**2.0**	**1.5**	**1.0**	**Less than 1.0**
Malaysia (910-920 MHz)	x	x	x	x	x	x	x	x	x	x	x	x	x	0.2700
Thailand (920-925 MHz)	x	x	x	x	x	x	x	x	x	x	x	x	x	0.2800
Indonesia (923-925 MHz)	x	x	x	x	x	x	x	x	x	x	x	x	x	0.2800
Singapore (920-925 MHz)	x	x	x	x	x	x	x	x	x	x	x	x	x	0.2600
Vietnam (920-923 MHz)	x	x	x	x	x	x	x	x	x	x	x	x	x	0.2700
United States (902-928 MHz)	x	x	x	x	x	x	x	x	x	x	x	x	x	0.2800
Total Average	0.2733 meter													

Table 6 Overweight BMI condition open-field experiment

No.	Read Range Distance (meter)													
	7.0	**6.5**	**6.0**	**5.5**	**5.0**	**4.5**	**4**	**3.5**	**3.0**	**2.5**	**2.0**	**1.5**	**1.0**	**Less than 1.0**
Malaysia (910-920 MHz)	x	x	x	x	x	x	x	x	x	x	x	x	x	0.1600
Thailand (920-925 MHz)	x	x	x	x	x	x	x	x	x	x	x	x	x	0.1700
Indonesia (923-925 MHz)	x	x	x	x	x	x	x	x	x	x	x	x	x	0.1700
Singapore (920-925 MHz)	x	x	x	x	x	x	x	x	x	x	x	x	x	0.1700
Vietnam (920-923 MHz)	x	x	x	x	x	x	x	x	x	x	x	x	x	0.2000
United States (902-928 MHz)	x	x	x	x	x	x	x	x	x	x	x	x	x	0.1900
Total Average	0.1766 meter													

Table 7 Obese BMI condition open-field experiment

No.	Read Range Distance (meter)													
	7.0	**6.5**	**6.0**	**5.5**	**5.0**	**4.5**	**4.0**	**3.5**	**3.0**	**2.5**	**2.0**	**1.5**	**1.0**	**Less than 1.0**
Malaysia (910-920 MHz)	x	x	x	x	x	x	x	x	x	x	x	x	x	0.1100
Thailand (920-925 MHz)	x	x	x	x	x	x	x	x	x	x	x	x	x	0.1100
Indonesia (923-925 MHz)	x	x	x	x	x	x	x	x	x	x	x	x	x	0.1100
Singapore (920-925 MHz)	x	x	x	x	x	x	x	x	x	x	x	x	x	0.1200
Vietnam (920-923 MHz)	x	x	x	x	x	x	x	x	x	x	x	x	x	0.1100
United States (902-928 MHz)	x	x	x	x	x	x	x	x	x	x	x	x	x	0.1500
Total Average	0.1183 meter													

When considering the presence of barriers like the human body, metal, or other conductive materials, the RR extension in free space can be significantly affected. Additionally, the variance in frequency ranges between different nations may result in slight changes in RR reading performance.

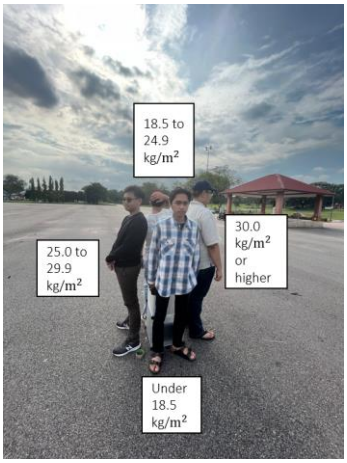

Fig.9 Graph of simulated read range in free space condition

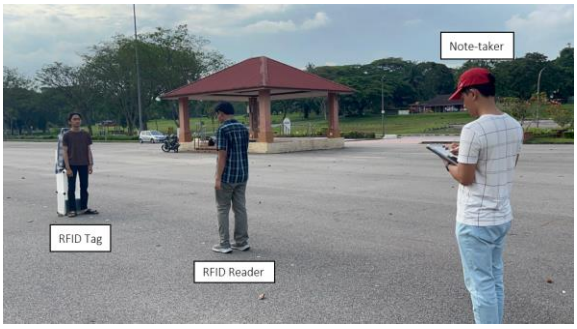

Fig.10 Open-field experiment process

CONCLUSION

The attachment of RFID tags under varying BMI conditions presented unique challenges. In the simulated read range using interference-free environment, the performance of an RFID tag can be reached up to 5.3 meters in free space without any signal interference that could diminish read range (RR) performances. The fat layer within the human body was found to influence the performance of RFID tag in terms of RR. The BMI categories of underweight, normal overweight, and obese were used as part of the experiment parameter. An open field experiment was conducted to investigate RR in a real-world setting. Under free space conditions, the RR could reach up to 6 meters. However, the read range performance decreased as the thickness of the body's fat layer increased. Underweight conditions exhibited a significant reduction in RR performance, reaching as low as 0.33 meter, representing a 179% decrease compared to the performance in free-space condition. For individuals with a normal BMI, the RR performance showed a reduction of 0.27 meters, corresponding to a 182% decrease. In the overweight condition, the RR decreased by 188%, reaching 0.1766 meter. The greatest reduction in RR performance compared to free space conditions was observed in the obese category, with a 192% decrease (0.1183 meter). The read range demonstrated efficient performance in the free space condition without any interference from materials such as metal, the human body, or other conductive substances. However, the performance was reduced due to variations in BMI conditions. The higher thickness, permittivity, and conductivity of the abdominal tissue layer contributed to the reduction in RR performance.

ACKNOWLEDGMENT

The authors would like to thank the Ministry of Higher Education (MOHE), School of Postgraduate Studies (SPS), Research Management Centre, Advanced Diagnostics and Progressive Human Care Research Group, Faculty of Electrical Engineering and Universiti Teknologi Malaysia (UTM), Johor Bahru, for the support of the research under Fundamental Research Grant Scheme FRGS/1/2023/TK07/UTM/02/23 and UTM Encouragement Research Grant Q.J130000.3851.20J74.

REFERENCES

Ahmed, S., Qureshi, S. T., Sydanheimo, L., Ukkonen, L., & Bjorninen, T. 2019. Comparison of Wearable E-Textile Split Ring Resonator and Slotted Patch RFID Reader Antennas Embedded in Work Gloves. IEEE Journal of Radio Frequency Identification, 3(4), 259-264. doi:10.1109/jrfid.2019.2926194

Bansal, A., Sharma, S., & Khanna, R. 2022. RFID Tag Design with high read range Performance for Dual band Applications in UHF Range. Paper presented at the 2022 IEEE 12th International Conference on RFID Technology and Applications (RFID-TA).

Bo Yin, M. Y., Youhai Yu. 2021. A Novel Compact Wearable Antenna Design for ISM Band. Progress In Electromagnetics Research C, 107, 97-111. doi:10.2528/PIERC20101901

Casula, G., & Montisci, G. 2019. A Design Rule to Reduce the Human Body Effect on Wearable PIFA Antennas. Electronics, 8(2). doi:10.3390/electronics8020244

Chainway. (n.d.). C72 UHF RFID Reader. Retrieved from https://www.richrfid.com/rfid-uhf-alien-9662-adhesive-label.html

Chatterjee, A., Gerdes, M. W., & Martinez, S. G. 2020. Identification of Risk Factors Associated with Obesity and Overweight-A Machine Learning Overview. Sensors (Basel), 20(9). doi:10.3390/s20092734

Chu H, K. J., Park S, Kim J, Lee JH, Ha WB, Jung HJ, Yang SB, Kim CH, Park JY, Kang KH, Lee S, Lee S. 2022. An Observational Study Using Ultrasound to Assess Allowable Needle Insertion Range of Acupoint CV12. Healthcare (Basel), 10(9). doi:10.3390/healthcare10091707

Farahat, A. E., Hussein, K. F. A. 2021. Wearable Button-Like Dual-Band Central Antenna for Wireless Bodyarea Networks. Progress In Electromagnetics Research B, 90, 21-41. doi:10.2528/PIERB20102007

Gao, M., & Lu, Y. 2022. URAP: a new ultra-lightweight RFID authentication protocol in passive RFID system. The Journal of Supercomputing, 78(8), 10893-10905. doi:10.1007/s11227-021-04252-y

Gmih, Y., & Farchi, A. 2020. Compact Antenna for UHF-RFID Tag Tested on the Human Body for Identification Cards. International Journal of Intelligent Engineering and Systems, 13(1), 227-236. doi:10.22266/ijies2020.0229.21

Jeong, S. M., Lee, D. H., Rezende, L. F. M., & Giovannucci, E. L. 2023. Different correlation of body mass index with body fatness and obesity-related biomarker according to age, sex and race-ethnicity. Sci Rep, 13(1), 3472. doi:10.1038/s41598-023-30527-w

Keshwani, V. R., Bhavarthe, P. P., & Rathod, S. S. 2021. Eight Shape Electromagnetic Band Spacing gap Structure for Bandwidth Improvement of Wearable Antenna. Progress In Electromagnetics Research C, 116, 37-49. doi:10.2528/PIERC21070603

Limited, A. T. 2024. Worldwide UHF RFID Frequency Allocations. Retrieved from https://airpluxtec.com/worldwide-uhf-rfid-frequency-allocations/

Miozzi, C., Amato, F., & Marrocco, G., 2020. Performance and Durability of Thread Antennas as Stretchable Epidermal UHF RFID Tags. IEEE Journal of Radio Frequency Identification, 4, 398-405. doi:10.1109/jrfid.2020.3001692

Miswadi, N., Abd Rahman, N., Subahir, S., Aris, M. A., Awang, R. E., & Lim, E. H. 2022. Design of a Flexible T-Matched Feed UHF RFID Tag Antenna. Journal of Physics: Conference Series. doi:10.1088/1742-6596/2250/1/012015

Mohajan, D., & Mohajan, H. K. 2023. Body Mass Index (BMI) is a Popular Anthropometric Tool to Measure Obesity Among Adults. Journal of Innovations in Medical Research, 2(4), 25-33. doi:10.56397/jimr/2023.04.06

Mohammad, G. B., Shitharth, S., Syed, S. A., Dugyala, R., Rao, K. S., Alenezi, F., Mustapha, A. 2022. Mechanism of Internet of Things (IoT) Integrated with Radio Frequency Identification (RFID) Technology for Healthcare System. Mathematical Problems in Engineering, 2022, 1-8. doi:10.1155/2022/4167700

Nie, H.K., Xuan, X.W., & Ren, G.J. 2021. Wearable antenna pressure sensor with electromagnetic bandgap for elderly fall monitoring. AEU - International Journal of Electronics and Communications, 138. doi:10.1016/j.aeue.2021.153861

RichAfid. (n.d.). RFID UHF 9662 Adhesive Label. Retrieved from https://www.richrfid.com/rfid-uhf-alien-9662-adhesive-label.html

Sakai, K., Nursetia, P., Sejati, P. A., Wicaksono, R., Hayashi, H., & Takei, M. 2023. Gastric functional monitoring by gastric electrical impedance tomography (gEIT) suit with dual-step fuzzy clustering. Sci Rep, 13(1), 514. doi:10.1038/s41598-022-27060-7

Soeroto AY, S. N., Purwiga A, Santoso P, Kulsum ID, Suryadinata H, Ferdian F. 2020. Effect of increased BMI and obesity on the outcome of COVID-19 adult patients: A systematic review and meta-analysis. Diabetes Metab Syndr, 14(6), 1897-1904. doi:10.1016/j.dsx.2020.09.029

Stopforth, C. P.-P. a. R. 2021. Radio frequency identification (RFID) stock control and geo-location data system from a moving vehicle. *Journal of Engineering, Design and Technology*. doi: 10.1108/jedt-10-2021-0548

Suryanata, F. A., Sim, M. S., Salem, B. A., Dewan, R., & You, K. Y. 2023. Effect of Human Body to the Read Range of Radio Frequency Identification. *Journal of Medical Devices Technology, 2*(1), 12-18. doi:https://doi.org/10.11113/jmeditec.v1n1.23

Suryanata, F. A. 2023. *Read Range Analysis of RFID Tag Under Human Proximity With Different Body Mass Index.* (Engineering). Universiti Teknologi Malaysia

Tajin M, A. C., Dion G, Dandekar K. 2021. Passive UHF RFID-Based Knitted Wearable. *IEEE Internet of Things Journal, 8*(17), 13763-13773. doi:10.1109/JIOT.2021.3068198

Technologies, B. 2022. What frequencies does RFID technology use and the reason why and to serve a range of applications and purpose for each. *News, Technology.* Retrieved from https://www.barcode-uk.com/insight/what-frequencies-does-rfid-technology-use-and-the-reason-why-and-to-serve-a-range-of-applications-and-purpose-for-each-/news%2Ctechnology#:~:text=use%20frequency%20920%2D925%20MHz,%2C%20Singapore%2C%20Thailand%2C%20etc.

Tsalapati, E., Tribe, J., Goodall, P. A., Young, R. I., Jackson, T. W., & West, A. A. 2021. Enhancing RFID system configuration through semantic modelling. *The Knowledge Engineering Review*(36).

Wissem El May, I. S., Jean Marc Ribero, Lotfi Osman. 2021. Design of Low-Profile and Safe Low SAR Tri-Band Textile EBG-Based Antenna for IoT Applications. *Progress In Electromagnetics Research Letters, 98*, 85-94. doi:10.2528/PIERL21051107

Xiang, J., Zhao, A., Tian, G. Y., Woo, W., Liu, L., Li, H., & Singh, P. K. 2022. Prospective RFID Sensors for the IoT Healthcare System. *Journal of Sensors, 2022*, 1-19. doi:10.1155/2022/8787275

Xu, J., Li, Z., Zhang, K., Yang, J., Gao, N., Zhang, Z., & Meng, Z. 2023. The Principle, Methods and Recent Progress in RFID Positioning Techniques: A Review. *IEEE Journal of Radio Frequency Identification, 7*, 50-63. doi:10.1109/jrfid.2022.3233855

Yalduz, H., Tabaru, T. E., Kilic, V. T., & Turkmen, M. 2020. Design and analysis of low profile and low SAR full-textile UWB wearable antenna with metamaterial for WBAN applications. *AEU - International Journal of Electronics and Communications, 126*. doi:10.1016/j.aeue.2020.153465